Quasi-one-dimensional optical lattices for soliton manipulation

Servando Lopez-Aguayo,[1,*] Cesar Ruelas-Valdez,[1] Benjamin Perez-Garcia,[1] Antonio Ortiz-Ambriz,[2] Raul I. Hernandez-Aranda,[1] and Julio C. Gutiérrez-Vega[1]

[1]*Photonics and Mathematical Optics Group, Tecnológico de Monterrey, Monterrey 64849, Mexico*

[2]*Estructura i Constituents de la Matèria, Universitat de Barcelona, Avenida Diagonal 647, 08028 Barcelona, Spain*

**Corresponding author: servando@itesm.mx*

Received August 5, 2014; revised October 10, 2014; accepted October 12, 2014; posted October 17, 2014 (Doc. ID 220491); published November 14, 2014

Based on angular spectrum engineering, we report the generation of optical lattices whose two-dimensional transverse nondiffracting pattern can be reduced to a quasi-one-dimensional intensity structure formed by either a single or multiple parallel channels. Remarkably, many features for each channel such as its maximum intensity, modulation, width, or separation among channels, can be controlled and modified in order to meet the requirements of particular applications. In particular, we demonstrate that these lattices can provide useful schemes for soliton routing and steering. We demonstrate the existence domain of ground-state solitons for the single quasi-one-dimensional lattice, and we show that these nondiffracting beams allow "push and pull" dynamics among the neighbor solitons propagated along the nondiffracting channels generated.

OCIS codes: (140.3300) Laser beam shaping; (260.1960) Diffraction theory; (190.6135) Spatial solitons.
http://dx.doi.org/10.1364/OL.39.006545

Transverse modulation in media where optical radiation is propagated and guided offers an abundance of interesting phenomena, which find applications in diverse fields such as trapping in Bose–Einstein condensation [1], micro-manipulation in optical tweezers [2], or colloidal particles in biophysics [3]. In particular, transverse modulation of refractive index can produce a wide range of phenomena in guiding optical solitons, in addition to the effects produced by diffraction and nonlinearities [4]. Previous works demonstrate experimentally the observation of solitons in optically induced nonlinear photonic lattices [5] and their potential for all-optical routing and switching [6]. The optical lattice induction technique is especially attractive because it allows producing reconfigurable index profiles. In order to maximize beam control, photoinduced lattice must remain invariant along the propagation direction [7] being hence the nondiffracting beams [8–10], ideal and natural candidates to produce the optical lattices required.

In this report, we use an approach based on angular-spectrum engineering to generate two-dimensional nondiffracting beams whose transverse intensity distribution can be reduced to a quasi-one-dimensional structure, allowing the generation of either single or multiple parallel channels. Remarkably, we show that it is suitable to control several parameters of these lattices, such as the required number and the separation among channels as well as the maximum amplitude imposed along the channels, the modulation, and the width of each channel. Finally, we show these lattices can open new schemes in routing and guiding solitons for future all-optical devices.

We consider propagation of optical radiation along the ξ axis in a biased photorefractive crystal. In the transverse coordinates η and ς, a periodic index modulation is optically induced. To allow the nonlinearity of the crystal to involve just the probe beam, we propagate orthogonally polarized to each other, the probe beam, and the optical lattice induced [7]. The propagation of the complex field amplitude q is described by the dimensionless nonlinear Schrödinger equation [7,11]

$$i\frac{\partial q}{\partial \xi}+\frac{1}{2}\left(\frac{\partial^2 q}{\partial \eta^2}+\frac{\partial^2 q}{\partial \varsigma^2}\right)+\frac{Eq[s|q|^2+R(\eta,\varsigma,\xi)]}{1+s|q|^2+R(\eta,\varsigma,\xi)}=0, \quad (1)$$

where the longitudinal ξ and transverse coordinates η and ς, are normalized to the diffraction length and to the input beam width, respectively, s stands for the saturation parameter, E represents the biasing static field applied to the photorefractive crystal, and the function $R(\eta,\varsigma,\xi)$ stands for the profile of the optical lattice induced. Equation (1) allows some conserved quantities such as the energy flow $U=\int_{-\infty}^{+\infty}\int_{-\infty}^{+\infty}|q|^2 d\eta d\varsigma$. We set $E=12$ and $s=0.2$. The parameters used in this report correspond to an input beam with ∼10 μm at the wavelength 633 nm, that is propagated into a SBN crystal biased with a static electric field of $\sim 10^6$ V/m and effective electro-optic coefficient of $\sim 1.8\times 10^{-10}$ m/V [5,11].

To date, many efforts have been done to study spatial solitons where the function $R(\eta,\varsigma,\xi)$ is an exact and basic solution of the linear Helmholtz equation [12]. Group theory demonstrates there are only four coordinate systems where the Helmholtz equation can be separable into their longitudinal and transversal components [13], allowing invariant solutions along the ξ axis: plane waves in Cartesian coordinates, Bessel beams in circular cylindrical coordinates [8], Mathieu beams in elliptic cylindrical coordinates [9], and parabolic beams in parabolic cylindrical coordinates [10]. Several studies of soliton propagation in the four nondiffracting beam families have been done using these families of nondiffracting beams [14–19]. An alternative form to express a nondiffracting beam is via the Whittaker integral $R(\eta,\varsigma,\xi)=W(\eta,\varsigma)\exp(-ik_z\xi)$ [4], where

$$W(\eta,\varsigma)=\int_0^{2\pi} G(\varphi)\exp[ik_t(\eta\cos\varphi+\varsigma\sin\varphi)]d\varphi, \quad (2)$$

here the longitudinal k_z and transverse k_t components of the k wave vector satisfy the expression, $k^2=k_z^2+k_t^2$, φ is the azimuth angle in frequency space, and $G(\varphi)$ is the

angular spectrum of the nondiffracting beam that in Eq. (2) is restricted to be localized in a ring of radius k_t. We set $\max[R(\eta,\varsigma,\xi)]=1$.

Motivated by the numerical results previously obtained with an iterative Fourier method to obtain arbitrary quasi-nondiffracting beams [20,21], we study the simple case when the angular spectrum is given analytically by a boxcar function $\Pi(\varphi)$, where

$$G(\varphi)\equiv\Pi(\varphi)=\begin{cases}\mu, & 0\le\varphi\le\nu,\\ 0, & \text{elsewhere},\end{cases}\tag{3}$$

here μ is a real constant and $\nu=2\pi\delta/100$ where $\delta\in(0,100]$. Setting $\delta=100$ and $\mu=1$ generates the well-known nondiffracting beam $R(\eta,\varsigma,\xi)=J_0(k_t\sqrt{\eta^2+\varsigma^2})\exp(-ik_z\xi)$, where J_0 is the zero-order Bessel function [8]. For $\delta=50$, a pattern that resembles an even parabolic beam [10] is generated. However in this report, we are interested to report the case when $\delta\to 0$, because then the Eq. (2) can be rewritten as

$$R(\eta,\varsigma,\xi)=\mu\nu\,\mathrm{sinc}\left(\frac{k_t\nu\varsigma}{2}\right)\times\exp\left[ik_t\left(\eta+\frac{v\varsigma}{2}-\frac{k_z}{k_t}\xi\right)\right]+O(\varphi^2),\tag{4}$$

where $\mathrm{sinc}(x)=\sin(x)/x$ and $O(\varphi^2)$ is the contribution of second and higher terms in a series expansion of $\cos(\varphi)$ and $\sin(\varphi)$ in Eq. (2). Note that for $\delta\to 0$, the transverse intensity of the optical pattern generated can be approximated to a function whose intensity depends only of the single spatial coordinate ς, and thus, these two-dimensional nondiffracting beams have a quasi-one-dimensional structure, but with a lower and different spatial frequency than the originally unique k_t.

In Fig. 1(a), we show the optical pattern obtained directly evaluating Eq. (2) using $\delta=3$; in this case, a considerable modulation along the channel is generated, i.e., there is a maximum amplitude located at the center of the channel, while there are minima amplitudes located at both extremes along the channel generated. This modulation can be practically smoothed out, generating a channel of constant amplitude, if δ is decreased as it is shown in Fig. 1(b). However, then the channel generated becomes wider. This trade-off between the modulation along the channel and their width can also be rescaled by modifying the corresponding k_t value.

Due to the quasi-one-dimensional structure of Eq. (4), we can use the space-shifting property of the Fourier transform [22], in order to generate m-multiple channels into the lattice generated as we set $G(\varphi)=\sum_{n=1}^{m}a_n\exp(ib_nk_t\cos\varphi)\Pi(\varphi)$, where a_n is a complex number that controls the maximum amplitude and the degree of interference among the n-channel with the rest of channels, and b_n is a real number that produces a shift of the channel into the space domain $R(\eta,\varsigma-b_n,\xi)$. Adjusting the a_n and b_n coefficients by using standard multi-variable optimization procedures [23], it is possible to generate a large variety of quasi-one-dimensional patterns. As an example, we set $m=4$ to generate a quasi-one-dimensional lattice with four parallel channels, as it is shown in Fig. 1(c). By adjusting again the a_n and b_n coefficients, it is also possible to switch off any of the four channels [Fig. 1(d)]. In a similar way, different maximum intensities for each of the four channels can also be selected at convenience [Fig. 1(e)], or it is possible to generate channels with different widths [Fig. 1(f)].

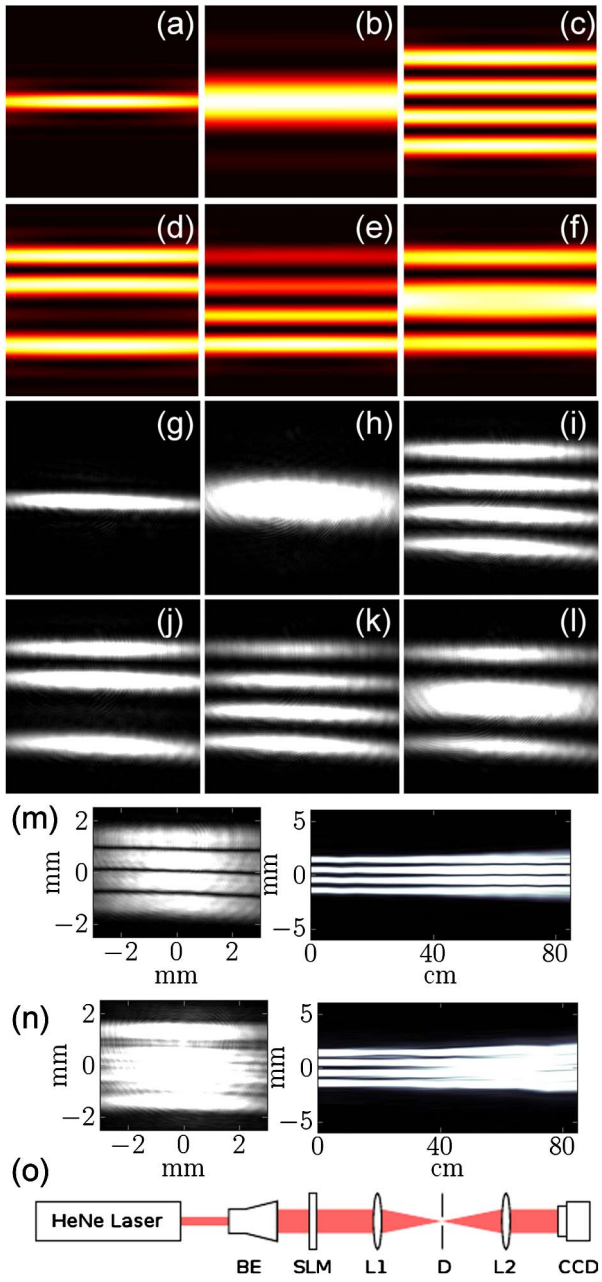

Fig. 1. Theoretical profiles of quasi-one-dimensional lattices with dimensionless parameters: (a) $\delta=3$, (b) $\delta=1$, (c) $\delta=2.5$, $a_n=\{-1.25,1,-1,1.25\}$, $b_n=\{1.08,0.36,-0.36,-1.08\}\cdot 10^{-2}$, (d) $\delta=2.5$, $a_n=\{1.2,1.1,-1\}$, $b_n=\{1.08,0.36,-0.36,-1.08\}\cdot 10^{-2}$, (e) $\delta=2.5$, $a_n=\{1,-1.1,1.3,-1.75\}$, $b_n=\{1.08,0.36,-0.36,-1.08\}\cdot 10^{-2}$, (f) $\delta=2.5$, $a_n=\{-1,1,1,-1\}$, $b_n=\{1.07,0.21,-0.21,-1.07\}\cdot 10^{-2}$. All profiles are shown in a $\eta-\varsigma$ box of about 0.0456 and using a $k_t=9,230$. (g)–(l) Corresponding experimental profiles. Longitudinal evolution of (m) a quasi-one-dimensional beam and (n) a similar beam in intensity but with a constant phase. The first frame is transverse intensity profile at $z=70$ cm (o) Experimental setup. He–Ne laser at 633 nm, 12 mW; BE, beam expander, 10x; SLM, spatial light modulator, LC2002; L1 and L2, lenses; D, diaphragm; CCD, Thorlabs CCD.

We demonstrate the feasibility of these quasi-one-dimensional beams using a transmissive spatial light modulator (SLM) with a resolution of 600×800 pixels. An image of the modulated pattern is sent to the SLM, which is then illuminated by a collimated plane wave from a He–Ne laser source. The angular spectrum of the modulated pattern coming out of the SLM is observed at the back focal plane of a positive lens of 500 mm focal length, then an iris diaphragm is employed to filter out all light not associated with the first diffraction order. This diaphragm is located at the front focal plane of a second lens of 300 mm focal length, which allows the generation of the desired nondiffracting pattern. The transverse intensity profiles of this beam were recorded using a CCD at different planes along the axis of propagation, for over a distance of 80 cm. We used a separation distance of 5 cm between the planes at which the profiles were recorded. The experimental results are shown in Figs. 1(g)–1(l). In order to demonstrate their nondiffracting behavior, we show in Fig. 1(m) the experimental propagation of a quasi-one-dimensional lattice of four channels obtained using the angular spectrum given by Eq. (3), and we compare it with a propagation of a similar initial intensity pattern, but using instead a pure constant phase distribution [Fig. 1(n)].

Next, we demonstrate that the lattices here generated can provide useful schemes for soliton routing and steering. Thus, we look for the ground-state soliton solutions of Eq. (1) in the form of $q(\eta, \varsigma, \xi) = w(\eta, \varsigma)\exp(ib\xi)$ where b is the soliton propagation constant. In general, we find that for lower b values, solitons are strongly elongated along the lattice channel, taking an elliptical shape, while higher b values produce solitons with a more circular shape.

The energy flow versus the soliton propagation constant is a monotonically increasing function as it is shown in Fig. 2(a). We have analyzed solitons obtained in a single channel using different δ values. According to the Vakithov–Kolokolov stability criterion [24], all these solitons obtained should be stable.

To study that the lattices allow the propagation of solitons along their channels, we impose an initial phase tilt α into the solitons previously obtained in the form of $q(\eta, \varsigma, \xi)\exp(i\alpha\eta)$. Note that modulation parameter δ generates a potential barrier capable to trap the moving solitons. In order to quantify this potential barrier, we calculate the critical angle α_{cr}, defined as the minimum tilt necessary by the solitons to overcome this potential barrier.

Hence, for $\alpha > \alpha_{\mathrm{cr}}$, tilted solitons fly apart from the center of the lattice, moving and escaping along the channel previously generated, while solitons with lower tilts than α_{cr}, remains trapped into the generated lattice, bouncing between two points of the channel's intensity. The critical tilt value is almost a linear decreasing function of the soliton propagation constant, as it is shown in Fig. 2(b). Higher energy flow values allows the launched solitons to overcome more easily the potential barrier of the optical lattice [Fig. 2(c)]. Note that solitons with higher soliton propagation constants propagating along channels with lower modulation require a lower critical tilt as it is shown in Fig. 2(d).

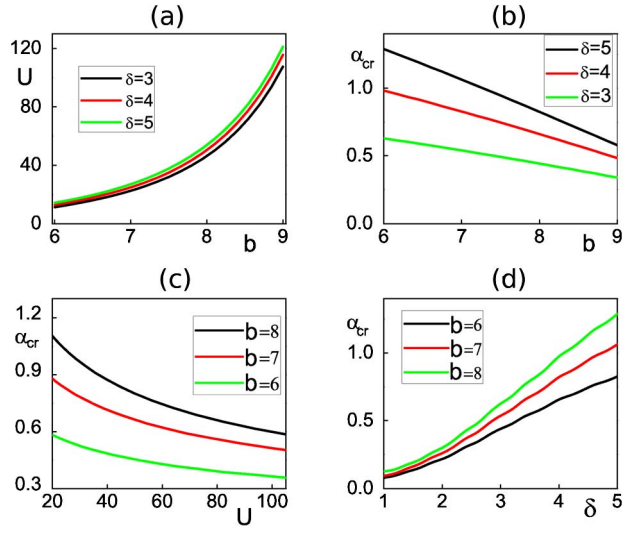

Fig. 2. Properties of ground-state solitons in quasi-one-dimensional lattices with single channel. (a) Energy flow versus propagation constant. (b) Critical tilt versus propagation constant. (c) Critical tilt of the solitons versus energy flow. (d) Critical tilt versus modulation parameter. In all cases, $k_t = 20$.

The optical lattices here reported, allow the possibility to design and control many schemes of soliton routing and steering. As an example, in Fig. 3(a) is shown how four solitons with different tilts can propagate along a quasi-one-dimensional lattice with four channels. Because for the four solitons the condition $\alpha < \alpha_{\mathrm{cr}}$ is fulfilled, all these solitons reverse their initial direction

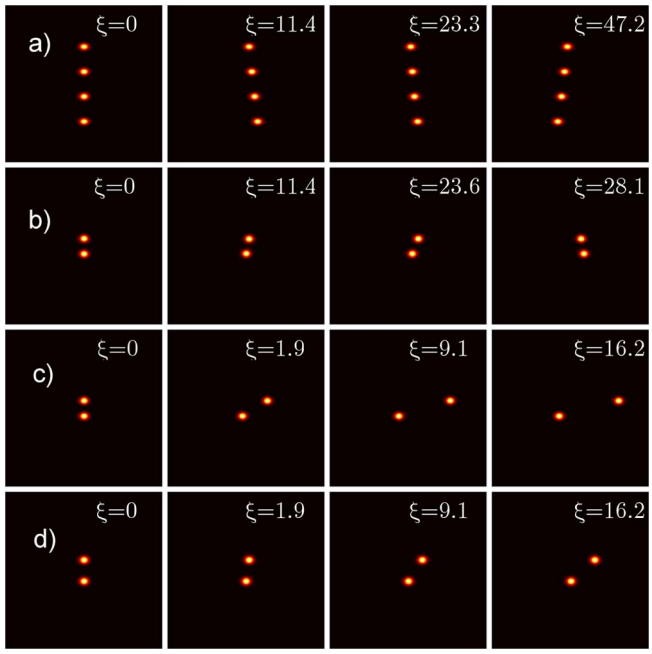

Fig. 3. Transverse dynamics of ground-state solitons propagated along quasi-one-dimensioal lattices with dimensionless parameters: (a) $b = 6$, $a_n = \{1, -1, 1, -1\}$, $b_n = \{5.85, 1.95, -1.95, -5.85\}$, $\alpha_n = \{0.05, 0.1, 0.15, 0.2\}$. (b) $b = 7$, $a_n = \{1, -1\}$, $b_n = \{1.25, -1.25\}$, $\alpha_n = \{0.25, 0\}$, both solitons are in phase. (c) $b = 7$, $a_n = \{1, -1\}$, $b_n = \{1.25, -1.25\}$, $\alpha_n = \{0.25, 0\}$, both solitons are out-phase. (d) $b = 7$, $a_n = \{1, -1\}$, $b_n = \{1.875, -1.875\}$, $\alpha_n = \{0.25, 0\}$. In all cases, $k_t = 20$. All the profiles are shown in a $\eta - \varsigma$ box of about 25 and using a $k_t = 20$.

of displacement. These dynamics arise from the interplay between the attracting force of the maximum intensity of the channel located at the center, and the transverse momentum and power imprinted to the solitons. Besides the possibility to control individually every soliton launched, it is possible to generate cross-interactions among the solitons of neighbor channels. These interactions can depend strongly on the soliton's relative phase. We show in Figs. 3(b) and 3(c) the propagation of solitons with the same power and the same initial tilt, but launching them with either the same or opposite phase, respectively. In the case of in-phase, the soliton of the upper channel starts to move, but then stop its movement due to the attractive potential experimented with the other soliton, while the second soliton, initially at rest, gains momentum and starts to move along the lattice channel. For the case of solitons out-phase, there is a repulsion force that produces the soliton initially at rest, moves into the opposite direction to the other tilted soliton. Thus, these optical lattices allow controllable "push and pull" dynamics among neighbor solitons, as the similar nonlinear dynamics that were reported for the case of optical Bessel lattices [14]. These dynamics are due to the interactions among adjacent solitons, and thus the interactions can be reduced by just increasing the separation of the channels, as it is shown in Fig. 3(d). Note that in this case, both solitons propagate independently from each other, minimizing their interaction potential. Thus, the optical lattices here reported could be used as soliton router in function of their modulation, separation, soliton's tilt, and phase imposed.

Summarizing, we demonstrated theoretically and experimentally, based on angular spectrum engineering, that is possible to produce two-dimensional transverse nondiffracting beams whose transverse structure can be composed by either single or multiple quasi-one-dimensional channels, placed and modulated as it is required. We demonstrate theoretically that these nondiffracting beams can be useful to route solitons, allowing new applications and uses in the future of all optical technologies.

We acknowledge support from Consejo Nacional de Ciencia y Tecnología (grants 182005 and 158174) and from Tecnológico de Monterrey (CAT-141). We thank LabMEMs for computer facilities. S. Lopez-Aguayo thanks Y. V. Kartashov and C. Lopez-Mariscal for useful comments.

References

1. A. Trombettoni and A. Smerzi, Phys. Rev. Lett **86**, 2353 (2001).
2. V. Garcés-Chávez, D. McGloin, H. Melville, W. Sibbett, and K. Dholakia, Nature **419**, 145 (2002).
3. D. J. Carnegie, D. J. Stevenson, M. Mazilu, F. Gunn-Moore, and K. Dholakia, Opt. Express **16**, 10507 (2008).
4. Y. V. Kartashov, V. A. Vysloukh, and L. Torner, Prog. Opt. **52**, 63 (2009).
5. J. W. Fleischer, M. Segev, N. K. Efremidis, and D. N. Christodoulides, Nature **422**, 147 (2003).
6. D. N. Christodoulides, F. Lederer, and Y. Silberberg, Nature **424**, 817 (2003).
7. N. K. Efremidis, S. Sears, D. N. Christodoulides, J. W. Fleischer, and M. Segev, Phys. Rev. E **66**, 046602 (2002).
8. J. Durnin, J. J. Miceli, Jr., and J. H. Eberly, Phys. Rev. Lett. **58**, 1499 (1987).
9. J. C. Gutiérrez-Vega, M. D. Iturbe-Castillo, and S. Chávez-Cerda, Opt. Lett. **25**, 1493 (2000).
10. M. A. Bandres, J. C. Gutiérrez-Vega, and S. Chávez-Cerda, Opt. Lett. **29**, 44 (2004).
11. Y. V. Kartashov, L. Torner, and D. N. Christodoulides, Opt. Lett. **30**, 1378 (2005).
12. Y. V. Kartashov, V. A. Vysloukh, and L. Torner, Eur. J. Phys. Special Topics **173**, 87 (2009).
13. E. G. Kalnins and W. Miller, Jr., J. Math. Phys. **17**, 330 (1976).
14. Y. V. Kartashov, V. A. Vysloukh, and L. Torner, Phys. Rev. Lett. **93**, 093904 (2004).
15. R. Fischer, D. N. Neshev, S. Lopez-Aguayo, A. S. Desyatnikov, A. A. Sukhorukov, W. Krolikowski, and Y. S. Kivshar, Opt. Express **14**, 2825 (2006).
16. A. Ruelas, S. López-Aguayo, and J. C. Gutiérrez-Vega, Opt. Lett. **33**, 2785 (2008).
17. Y. V. Kartashov, A. A. Egorov, V. A. Vysloukh, and L. Torner, Opt. Lett. **31**, 238 (2006).
18. F. Ye, D. Mihalache, and B. Hu, Phys. Rev. A **79**, 053852 (2009).
19. Y. V. Kartashov, V. A. Vysloukh, and L. Torner, Opt. Lett. **33**, 141 (2008).
20. S. López-Aguayo, Y. V. Kartashov, V. A. Vysloukh, and L. Torner, Phys. Rev. Lett. **105**, 013902 (2010).
21. Y. V. Kartashov, S. López-Aguayo, V. A. Vysloukh, and L. Torner, Opt. Express **19**, 9505 (2011).
22. J. W. Goodman, *Introduction to Fourier Optics* (McGraw-Hill, 1968).
23. W. Press, B. Flannery, S. Teukolsky, and W. Vetterling, *Numerical Recipes in C* (Cambridge University, 2007).
24. N. G. Vakhitov and A. A. Kolokolov, Radiophys. Quantum Electron. **16**, 783 (1973).